Inorganica Chimica Acta 486 (2019) 757–765

Contents lists available at ScienceDirect

Inorganica Chimica Acta

journal homepage: www.elsevier.com/locate/ica

Research paper

Dioxidomolybdenum(VI) and dioxidouranium(VI) complexes as functional mimic of haloperoxidases catalytic activity in presence of H_2O_2–KBr–$HClO_4$

Mannar R. Maurya[a,*], Bekele Mengesha[a], Shailendra K. Maurya[a], Nidhi Sehrawat[a], Fernando Avecilla[b]

[a] Department of Chemistry, Indian Institute of Technology Roorkee, Roorkee 247667, India
[b] Grupo Xenomar, Centro de Investigacións Científicas Avanzadas (CICA), Departamento de Química, Facultade de Ciencias, Universidade da Coruña, Campus de A Coruña, 15071 A Coruña, Spain

ARTICLE INFO

Keywords:
Tetradentate ONNO donor Mannich base ligands
Dioxidomolybdenum (VI) complex
Dioxidouranium (VI) complex
Single crystal X-ray study
NMR spectroscopy
Oxidative bromination of thymol

ABSTRACT

The stable dibasic tetradentate ligand 1,4-bis-(2-hydroxy-3,5-dimethylbenzyl)piperazine (H_2pip-2,4-dmp, **I**) prepared by reacting 2,4-dimethylphenol with piperazine in the presence of formaldehyde reacts with $[Mo^{VI}O_2(acac)_2]$ and $[U^{VI}O_2(CH_3COO)_2]$ in equimolar ratio to give neutral *hexa*-coordinated $[Mo^{VI}O_2$(pip-2,4-dmp)] (**1**) and hepta-coordinated $[U^{VI}O_2$(pip-2,4-dmp)(MeOH)] (**2**), respectively. After characterizing these complexes by spectroscopic (IR, UV/Vis, ^{1}H and ^{13}C NMR) data, elemental and thermal analyses (and single crystal X-ray diffraction study of uranium complex), they are used as catalysts to study the oxidative bromination of thymol. Such catalytic reactions are observed by many model vanadium complexes and are considered as a functional mimic of haloperoxidases. The catalytic oxidation resulted in the formation of three products namely, 2-bromothymol, 4-bromothymol and 2,4-dibromothymol. The optimized reaction conditions are obtained considering concentration of KBr, $HClO_4$, and oxidant for the maximum yield of brominated products. Under the optimized reaction conditions, the product selectivity for both the prepared complexes is investigated. They are found to be competent homogeneous catalysts to afford the products in good yield.

1. Introduction

Molybdenum is an essential metal which is capable of forming complexes with many compounds of biological importance such as carbohydrates, amino acids and other bioinspired ligands [1–3]. These model complexes can catalyze a wide variety of biochemical reactions. The most commonly studied reactions (other than biochemical) in which dioxidomolybdenum(VI) complexes act as catalysts are epoxidation of alkenes [4–14], oxidation of alcohols [15,16] and sulfur based compounds [17–19], and oxidative halogenation of organic substrates [20–22]. The nature of complex, oxidant and reaction conditions decide whether the reaction will proceed via a homolytic or electrophilic oxidation. In current years artificial enzyme mimics have become a hot topic of research since they present many advantages over conventional enzymes, namely easier preparation, lower price and improved stability, overcoming the drawbacks of natural enzymes [23–25]. Dioxidomolybdenum(VI) complexes are air stable and show functional as well as structural similarity with vanadium based haloperoxidases, thus can be considered as artificial models for heloperoxidases [22,25,26].

Amongst the actinides, uranium is the only element being well known for their coordination chemistry. Like molybdenum, uranium in its *trans*-$[UO_2]$ form forms stable complexes in higher oxidation state [27,28] but their catalytic activities are not much explored [27–29]. Therefore, the objective of the present work is to prepare dioxidomolybdenum(VI) and dioxidouranium(VI) complexes of stable dibasic tetradentate ligand, 1,4-bis-(2-hydroxy-3,5-dimethylbenzyl)piperazine (abbreviated as H_2pip-2,4-dmp, Scheme 1) and study their catalytic activity as homogeneous catalysts for the oxidative bromination of thymol, an essential catalytic reaction observed by many model vanadium complexes [22,25,26]. It has been observed that both complexes mimic similar catalytic activity as shown by vanadium based haloperoxidases and show very good conversion of thymol to the corresponding oxidative brominated products.

* Corresponding author.
E-mail address: rkmanfcy@iitr.ac.in (M.R. Maurya).
URL: https://www.iitr.ac.in/CY/rkmanfcy (M.R. Maurya).

https://doi.org/10.1016/j.ica.2018.11.031
Received 18 September 2018; Received in revised form 21 November 2018; Accepted 21 November 2018
Available online 22 November 2018
0020-1693/

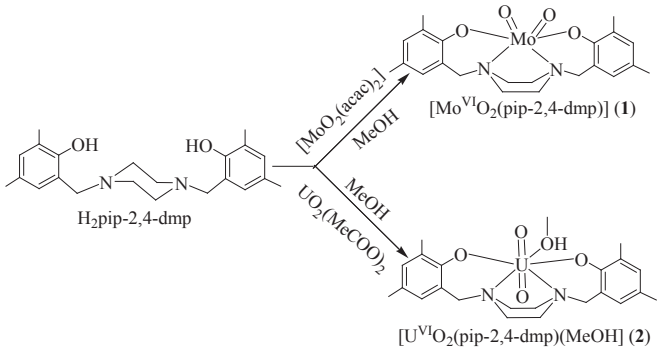

Scheme 1. Synthetic route to prepare [$Mo^{VI}O_2$(pip-2,4-dmp)] (**1**) and [$U^{VI}O_2$(pip-2,4-dmp)(MeOH)] (**2**).

2. Experimental

2.1. Materials

MoO_3 (S.D. fine, India), uranyl acetate dihydrate (Loba chemie, India), piperazine, 2,4-dimethylphenol (Aldrich Chemicals, USA) and thymol (Himedia, India) were used as obtained. [$Mo^{VI}O_2(acac)_2$] was prepared following the method reported in literature [30]. Ligand 1,4-bis-(2-hydroxy-3,5-dimethylbenzyl)piperazine (H_2pip-2,4-dmp) (**I**) was prepared following the method reported in literature [31]. All other chemicals and solvents used were of AR grade.

2.2. General procedures and techniques

Elemental (C, H and N) analysis of ligand and complexes were carried out on an elementar model Vario-E1-III. IR spectra were recorded as KBr pellets on a Nicolet 1100 FT-IR spectrometer. Electronic spectra of ligands and complexes were measured in MeCN with a Shimadzu 2600 UV–Vis spectrophotometers. The ^{1}H and ^{13}C NMR spectra of ligand and complexes were taken in $CDCl_3$/DMSO-d_6 using a JEOL ECX 400 MHz spectrometer. The thermogravimetric analysis of the complexes was carried out under oxygen atmosphere using a TG Stanton Redcroft STA 780 instrument. A Shimadzu 2010 plus gas-chromatograph fitted with an Rtx-1 capillary column (30 m × 0.25 mm × 0.25 μm) and a FID detector was used to analyze the reaction products and their quantification was made based of the relative peak area of each product. The identity of the products was confirmed using a GC–MS model Perkin-Elmer, Clarus 500 and comparing the fragments of each product with the library available.

2.3. Synthesis of [$Mo^{VI}O_2$(pip-2,4-dmp)] (1)

The ligand H_2pip-2,4-dmp (1.77 g, 5 mmol) was dissolved in 80 mL methanol by refluxing on a water bath for 2 h. A solution of [$Mo^{VI}O_2(acac)_2$] (1.625 g, 5 mmol) in methanol (15 mL) was added to the solution of ligand and the reaction mixture was allowed to reflux for 24 h, whereupon a yellow precipitate separated out. The solution volume was reduced to ca. 20 mL and the separated product was collected by filtration, washed with methanol and dried in vacuum desiccator. Yield: 33.1% (0.792 g) Cal. For $C_{22}H_{28}N_2O_4Mo$ (480); C, 55.0; H, 5.83; N, 5.83. Obs. C, 54.6; H, 5.9; N, 5.8%.

2.4. Synthesis of [$U^{VI}O_2$(pip-2,4-dmp)(MeOH)] (2)

A solution of [$U^{VI}O_2(CH_3COO)_2$]·$2H_2O$ (2.125 g, 5 mmol) in 10 mL methanol was added to the stirred solution of ligand (1.77 g, 5 mmol) in 80 mL MeOH prepared as mentioned above and the resulting reaction mixture was refluxed on a water bath for 24 h as a result of which a yellow-orange precipitate appeared. The solution volume was reduced to ca. 20 mL and the separated product was filtered, washed with methanol and dried in vacuuo. Yield: 40.8% (1.27 g). Cal. For $C_{22}H_{32}N_2O_5U$ (642); C, 41.12; H, 4.98; N, 4.36. Obs. C, 40.6; H, 4.9; N, 4.5%. Crystals of the complex suitable for X-ray study were grown in DMSO and obtained complex is now abbreviated as [$U^{VI}O_2$(pip-2,4-dmp)(DMSO)] (**2a**).

2.5. X-Ray crystal structure determination

Three-dimensional X-ray data of [$U^{VI}O_2$(pip-2,4-dmp)(DMSO)] (**2a**) were collected on a Bruker Kappa Apex CCD diffractometer at room temperature by the ϕ-ω scan method. Reflections were measured from a hemisphere of data collected from frames, each of them covering 0.3° in ω. A total of 26000 reflections measured were corrected for Lorentz and polarization effects and for absorption by multi-scan methods based on symmetry-equivalent and repeated reflections. Of the total, 5271 independent reflections exceeded the significance level ($|F|/\sigma|F|$) > 4.0. After data collection an empirical absorption correction (SADABS) [32] was applied, and the structure was solved by direct methods and refined by full matrix least-squares on F^2 data using SHELX suite of programs [33]. Hydrogen atoms were included in calculated position and refined in the riding mode, except for C(3), C(5) and C(16), which were located in difference Fourier map and freely refined. A final difference Fourier map showed no residual density outside: 0.912 and −0.668 e.Å^{-3} for **2a**. Due to disorder in DMSO molecule bonded to U(1) atom, two positions for sulfur atom of DMSO molecule were refined with anisotropic atomic displacement parameters. The site occupancy factor was 0.91716 for S(1A). A weighting scheme $w = 1/[\sigma^2(F_o^2) + (0.018900P)^2 + 2.237600P]$, where $P = (|F_o|^2 + 2|F_c|^2)/3$, was used in the latter stages of refinement. Further details of the crystal structure determination are given in Table 1. CCDC 1866906 contains the supplementary crystallographic data for the structure reported in this paper. These data can be obtained free of charge via http://www.ccdc.cam.ac.uk/conts/retrieving.html, or from the Cambridge Crystallographic Data Centre, 12 Union Road, Cambridge CB2 1EZ, UK; fax: (+44) 1223 336 033; or e-mail: deposit@ccdc.cam.ac.uk. Supplementary data associated with this article can be found, in the online version, at doi: 10.1016/j.ica.2018.11.031

Table 1
Crystal Data and Structure Refinement for [$U^{VI}O_2$(pip-2,4-dmp)(DMSO)] (**2a**).

Formula	$C_{24}H_{34}N_2O_5SU$
Formula weight	700.62
T, *K*	293(2)
Wavelength, Å	0.71073
Crystal system	Monoclinic
Space group	$P2_1/c$
a/Å	11.6974(10)
b/Å	14.5623(12)
c/Å	15.2257(12)
β/°	95.112(4)
V/Å^3	2583.2(4)
Z	4
F_{000}	1360
D_{calc}/g cm^{-3}	1.801
μ/mm^{-1}	6.400
θ/(°)	2.53 to 28.61
R_{int}	0.0292
Crystal size/mm^3	0.09 × 0.06 × 0.05
Goodness-of-fit on F^2	1.059
R_1[I > 2σ(I)][a]	0.0210
wR_2 (all data)[b]	0.0525
Largest differences peak and hole (eÅ^{-3})	0.912 and −0.668

[a] $R_1 = \Sigma||F_o| - |F_c|/\Sigma|F_o|$.
[b] $wR_2 = \{\Sigma[w(|F_o|^2 - |F_c|^2)^2]/\Sigma[w(F_o^2)^2]\}^{1/2}$.

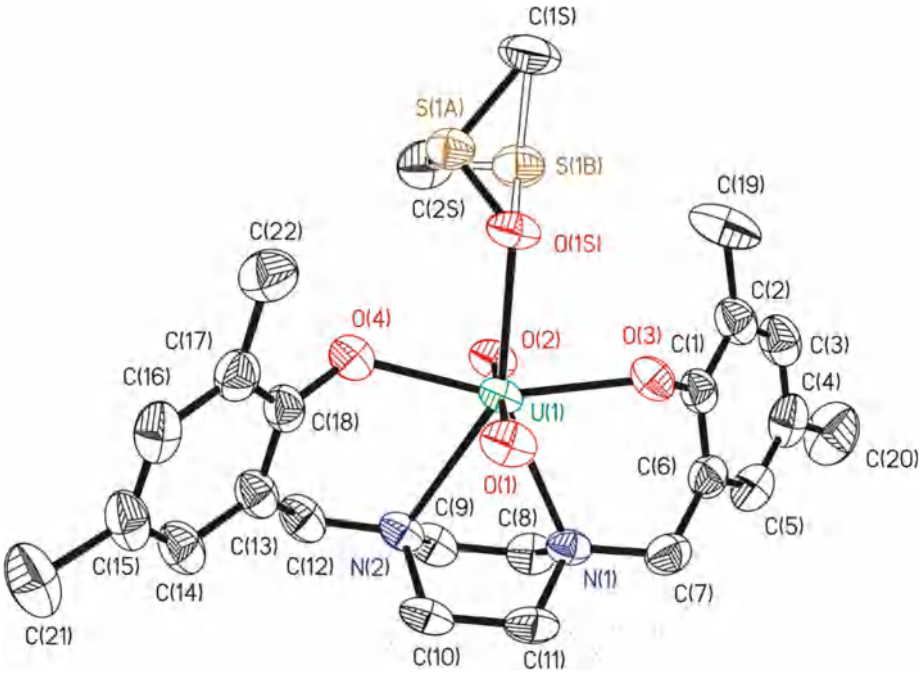

Fig. 1. ORTEP for the compound [$U^{VI}O_2$(pip-2,4-dmp)(DMSO)] (**2a**). All the non-hydrogen atoms are presented by their 50% probability ellipsoids. Hydrogen atoms are omitted for clarity.

2.6. Catalytic activity study: Oxidative bromination of thymol

All the reactions were carried out in a 100 mL two-necked round bottom flask. In a typical reaction, thymol (1.5 g, 10 mmol) and aqueous 30% H_2O_2 (1.13 g, 10 mmol) and KBr (1.19 g, 10 mmol) were added in 20 mL water. After adding the metal-complex (i.e. catalyst) (0.002 g), 70% $HClO_4$ (1.43 g, 10 mmol) was added to the reaction flask and the reaction mixture was stirred for 2 h at room temperature. The reaction mixture was then extracted with *n*-hexane where the products moved into the *n*-hexane layer. The oxidized products were analyzed quantitatively by withdrawing small aliquots from the *n*-hexane and subjected to GC and their quantifications were made on the basis of the relative peak area of the respective product. The obtained main products were further confirmed by ^{1}H NMR spectroscopy as well as GC–MS after their separations.

3. Results and discussion

A Mannich condensation between piperazine, 40% formaldehyde and 2,4-dimethyl phenol (1:2:2 M ratio) in refluxing MeOH yields the Mannich base ligands, H_2pip-2,4-dmp (**I**) in excellent yield [31]. Reaction of **I** with [$Mo^{VI}O_2$(acac)$_2$] and [$U^{VI}O_2$(CH_3COO)$_2$] in refluxing methanol resulted in the formation of [$Mo^{VI}O_2$(pip-2,4-dmp)] (**1**) (yellow) and [$U^{VI}O_2$(pip-2,4-dmp)(MeOH)] (**2**) (reddish-brown), respectively, as stable solid. Idealized structures of the complexes are shown in Scheme 1 which are based on the spectroscopic (IR, UV/Vis and ^{1}H NMR) data, elemental and thermal analyses, and X-ray diffraction study of [$U^{VI}O_2$(pip-2,4-dmp)(DMSO)] (**2a**, a DMSO coordinated complex **2**). Both complexes are soluble in methanol, dichloromethane, dimethyl sulfoxide and acetonitrile.

3.1. Thermogravimetric analysis study

Thermogravimetric analysis (TGA) profile of [$Mo^{VI}O_2$(pip-2,4-dmp)] (1) under an oxygen atmosphere shows a mass loss of ca. 2.0% between 60 and 100 °C which is possibly due to moisture or traces of water/methanol of crystallization. The complex is then stable up to ca. 200 °C. Above this temperature complex starts decomposing in three exothermic steps and stabilizes at ca. 500 °C. The obtained residue of 31.1% at this temperature is equivalent to the formation of stable MoO_3 (Cal for MoO_3 = 30%). The residue is stable up to 710 °C and then volatilizes beyond this temperature. TGA profile of [$U^{VI}O_2$(pip-2,4-dmp)(MeOH)] (**2**) shows a mass loss (Fig. S1) between 60 °C and 285 °C equivalent to 4.9% which is equal to one methanol (Cal. 4.98%) coordinated to uranium. Increasing temperature further, it decomposes in three exothermic steps and stabilizes at ca. 525 °C. The residue obtained (42.9%) at this temperature equals to U_3O_8 (Cal. 43.41%). This residue is stable up to 1000 °C.

3.2. Description of structure of [$U^{VI}O_2$(pip-2,4-dmp)(DMSO)] (2a)

Fig. 1. Selected bond distances and angles are given in Table 2. It is a mononuclear complex, which crystallizes in a monoclinic space group $P2_1/c$. The structure adopts a distorted pentagonal bipyramidal geometry around of metal centre. The ligand acts as tetradentate, coordinated through two phenoxido oxygen and two piperazine nitrogen atoms. The piperazine nitrogen atoms present a distorted sp^3 hybridized bonding network. U centre completes the coordination sphere by bonding to two O_{oxido} terminal oxygen atoms and one oxygen atom from solvent molecule (DMSO). The U=O bond lengths [1.788(2)–1.792(2) Å] are similar to other in the literature [34]. The two distances U=$O_{phenoxido}$ [2.225(2) and 2.234(2) Å] are shorter than the U=O_{DMSO} [2.446(2) Å] and are trans to each other. The equatorial plane is occupied by the $O_{phenoxido}$ atoms, O(3) and O(4), by the $N_{piperazine}$ atoms, N(1) and N(2) and by the oxygen atom (O1S) of DMSO molecule. They are distorted respect to the planarity, [mean deviation from the plane 0.0857(14) Å]. The terminal oxido atoms occupy the axial sites. The crystal packing (Fig. 2) does not present hydrogen bonds between the electronegative atoms. π-π Interactions are not present either.

3.3. IR spectral study

Table 3 presents IR spectral data of ligand and complexes. The ligand H_2pip-2,4-dmp exhibits a broad band at ca. 3440 cm^{-1} due to the υ(OH) of the phenol. Absence of this band in molybdenum complex

Table 2
Bond lengths [Å] and angles [°] for the compounds [$U^{VI}O_2$(pip-2,4-dmp)(DMSO)] (**2a**).

Bond lengths			
U(1)-O(1)	1.792(2)	N(1)-C(7)	1.481(4)
U(1)-O(2)	1.788(2)	N(1)-C(8)	1.477(4)
U(1)-O(3)	2.225(2)	N(1)-C(11)	1.479(4)
U(1)-O(4)	2.234(2)	N(2)-C(9)	1.485(4)
U(1)-O(1S)	2.446(2)	N(2)-C(10)	1.483(4)
U(1)-N(1)	2.640(3)	N(2)-C(12)	1.484(4)
U(1)-N(2)	2.639(2)		
Angles			
O(2)-U(1)-O(1)	176.48(10)	C(8)-N(1)-C(11)	107.0(2)
O(2)-U(1)-O(3)	89.86(9)	C(8)-N(1)-C(7)	110.5(3)
O(1)-U(1)-O(3)	90.88(10)	C(11)-N(1)-C(7)	109.8(2)
O(2)-U(1)-O(4)	91.25(10)	C(8)-N(1)-U(1)	106.85(18)
O(1)-U(1)-O(4)	89.33(10)	C(11)-N(1)-U(1)	105.69(19)
O(3)-U(1)-O(4)	158.26(9)	C(7)-N(1)-U(1)	116.45(19)
O(2)-U(1)-O(1S)	87.95(9)	C(10)-N(2)-C(12)	111.3(2)
O(1)-U(1)-O(1S)	95.56(9)	C(10)-N(2)-C(9)	106.9(3)
O(3)-U(1)-O(1S)	80.24(8)	C(12)-N(2)-C(9)	109.2(2)
O(4)-U(1)-O(1S)	78.10(8)	C(10)-N(2)-U(1)	106.16(17)
O(2)-U(1)-N(2)	84.44(9)	C(12)-N(2)-U(1)	116.3(2)
O(1)-U(1)-N(2)	92.42(9)	C(9)-N(2)-U(1)	106.40(18)
O(3)-U(1)-N(2)	128.86(8)		
O(4)-U(1)-N(2)	72.83(9)		
O(1S)-U(1)-N(2)	149.72(8)		
O(2)-U(1)-N(1)	87.82(9)		
O(1)-U(1)-N(1)	89.12(9)		
O(3)-U(1)-N(1)	72.60(8)		
O(4)-U(1)-N(1)	129.14(8)		
O(1S)-U(1)-N(1)	152.51(8)		
N(2)-U(1)-N(1)	56.46(8)		

suggests the deprotonation and coordination of phenolic oxygen to molybdenum while a weak band in the 3400 cm^{-1} region in uranium complex possibly suggests the presence of coordinated methanol. The presence of several medium intensity bands between 2500 and 2800 cm^{-1} in the ligand as well as in complexes suggest the existence of C–H stretching bands due to $-CH_2$. The υ(C–N) of ring nitrogen has no systematic trend in ligand and complexes. The presence of two sharp peaks in molybdenum complex at 944 and 906 cm^{-1} due to υ_{asym}(O=Mo=O) and υ_{sym}(O=Mo=O) stretches, respectively, confirm the presence of *cis*-[$Mo^{VI}O_2$] moiety. In uranium complex, one sharp band appears at 900 cm^{-1} and other one appears in the lower region at 859 cm^{-1}, due to υ_{asym}(O=U=O) and υ_{sym}(O=U=O), respectively, indicate the presence of *trans*-[$U^{VI}O_2$] structure. Thus, the spectral data confirms the coordination of the ligand to the metal in both complexes.

3.4. UV–Vis spectral study

Fig. S2 presents UV–visible spectra of ligand and complexes and Table 4 provides absorption maxima of ligands and complexes along with their extinction coefficients. The ligand shows three bands at 223, 286 and 330 nm in the UV region. Based on their molar extinction coefficient, the first band at 223 nm is assigned due to $\sigma \rightarrow \sigma^*$ transition whereas the band at 286 nm is due to $\pi \rightarrow \pi^*$ transition. The low intensity band at 330 nm is due to $n \rightarrow \pi^*$ transition. The 330 nm band shifts to higher wavelength i.e. at 353 and 389 nm in [$Mo^{VI}O_2$(Pip-2,4-dmp)] (**1**) and [$U^{VI}O_2$(pip-2,4-dmp)(MeOH)] (**2**), respectively. An additional band at 425 nm in **1** arises due to the ligand to metal charge transfer from the filled π orbital of ligand to the vacant d orbital of the metal while such band at 510 nm in **2** is due to $^{1\varepsilon}g^+ \rightarrow {}^3\pi_u$ transition [23].

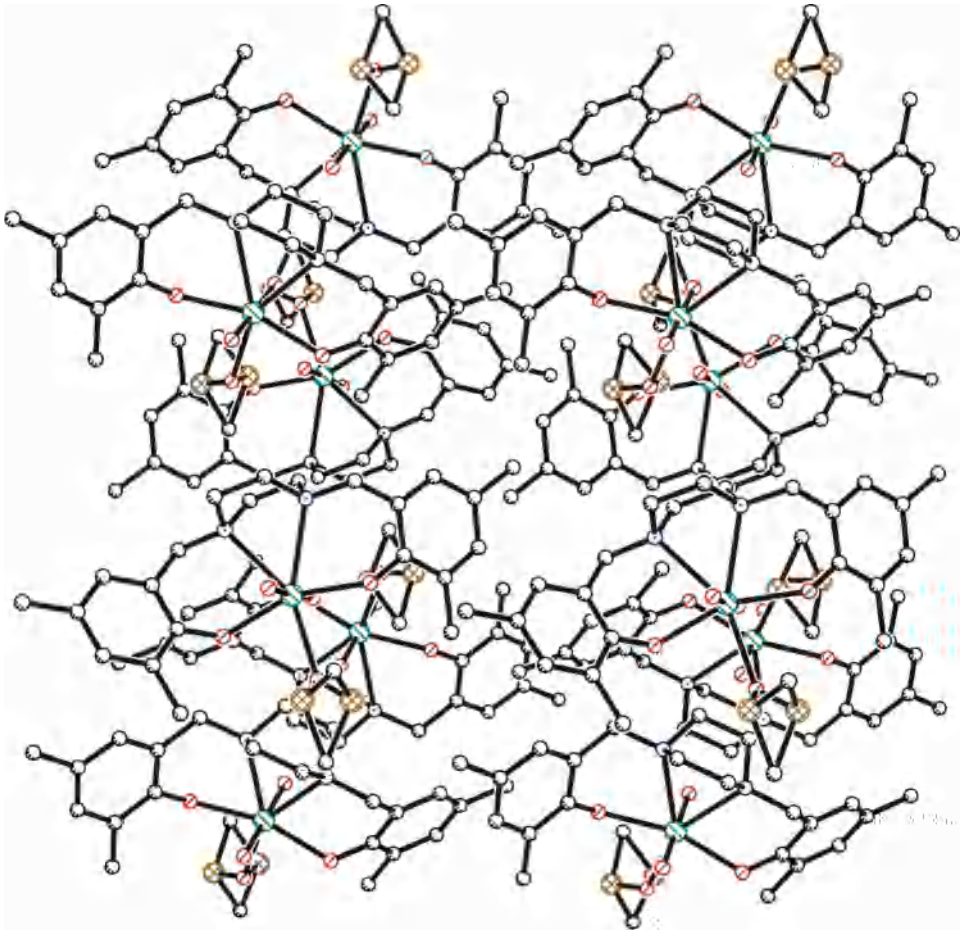

Fig. 2. Crystal packing of the compound [$U^{VI}O_2$(pip-2,4-dmp)(DMSO)] (**2a**). Drawing was done in balls and sticks using SHELXL package. Hydrogen atoms are omitted for clarity.

Table 3
IR spectral data (cm^{-1}) of ligand and complexes.

Compound	υ (O−H)	υ (C−N)	υ(CH_2)	υ_{asym} (O=M=O)	υ_{sym} (O=M=O)
H_2pip-2,4-dmp	3440	1156	2932		
[$Mo^{VI}O_2$(pip-2,4-dmp)]		1162	2923	944	906
[$U^{VI}O_2$(pip-2,4-dmp)(MeOH)]	3428	1150	2928	900	859

Table 4
UV–visible spectral data of ligand and complexes.

Compound	Solvent	λ (nm) (ε/$M^{-1}cm^{-1}$)
H_2Pip-2,4-dmp	MeOH	223(682), 286(1252), 330(370)
[$Mo^{VI}O_2$(pip-2,4-dmp)]	MeOH	291(2072), 353(51), 425(110)
[$U^{VI}O_2$(pip-2,4-dmp)(MeOH)]	MeOH	222(690), 284(1812), 389(399), 510(178)

Table 5
^{1}H NMR (δ in ppm) of ligand and metal complexes.

Compound	OH	Aromatic H	$-CH_2$	$-CH_3$	$-NCH_2$ (piprazine)
H_2pip-2,4-dmp	10.5 (2H)	6.63 (s, 2H), 6.87 (s, 2H)	3.66 (s, 4H)	2.21(s, 6H), 2.20(s, 6H)	2.67(s, 8H)
[$Mo^{VI}O_2$(pip-2,4-dmp)]	–	6.83 (s, 2H), 6.63 (s, 2H)	3.66 (s, 4H)	2.21(s, 6H), 2.19(s, 6H)	1.26(s, 8H)
[$U^{VI}O_2$(pip-2,4-dmp)(MeOH)]	–	6.84 (s, 2H), 6.72 (s, 2H)	3.68 (b, 4H)	2.10(s, 6H), 2.08(s, 6H)	2.15(s, 8H)

3.5. ^{1}H NMR spectral study

The ^{1}H NMR spectra of ligand and metal complexes were recorded in $CDCl_3$. The relevant spectral data are presented in Table 5 and spectra are accessible in the supporting information (Figs. S3–S5). Ligand **I** exhibits a broad band at 10.5 ppm due to phenolic protons and absence of this band in the spectra of complexes suggests the coordination of phenolic oxygen to the metal after proton replacement. An up field shift of signals due to –NCH_2 (piperazine) from 2.67 ppm (s, 8H) to 1.26 ppm (in **1**) and 2.15 ppm (in **2**) occurs which is possibly due to adjustment of ring current upon coordination of ring nitrogen to the metal. As expected signals due to aromatic, methylene and methyl protons are not much affected and appear at their expected positions.

3.6. ^{13}C NMR spectral study

We have also recorded ^{13}C NMR of ligand and complexes (Table 6) to ascertain the binding modes of the ligand towards complexes. The representative spectra (ligand and uranium complex) are presented in Fig. 3. The spectra recorded in DMSO-d_6 show considerable coordination–induced ^{13}C NMR chemical shifts {Δδ = [δ(complex) − δ(ligand)]} for those carbon atoms that are in the vicinity of the coordinating atoms like, C_1/C_1' (the carbon atoms close to phenolic oxygen), C_7/C_7' and C_8/C_8' (the carbon atoms close to the ring nitrogen). Even carbon atoms C_6/C_6' of benzene ring which are attached to C_7/C_7' are also affected. All these informations supplement the conclusion drawn from ^{1}H NMR data. Other signals of ligand and complexes appear well within the expected region. We could not observed the signal due to methyl carbon of coordinated methanol in complex **2**, possibly due to exchange of methanol with DMSO while recording the spectrum.

3.7. Catalytic activity study: oxidative bromination of thymol

The oxidative bromination of thymol catalyzed by the metal complexes has been carried out using KBr, 30% aqueous H_2O_2 and 70% aqueous $HClO_4$ in aqueous medium. Acid is required to proceed the reaction. The electrophilic aromatic substitution in the phenolic ring led the bromination of thymol and formation of two isomers, 2-bromothymol and 4-bromothymol and further bromination of the *ortho/para* isomer led the formation of 2,4-dibromothymol (Scheme 2). Among these products, 2,4-dibromothymol was found in the highest yield, possibly because of the further bromination of the monobromo product(s).

Table 6
^{13}C NMR data (δ in ppm) of ligand and metal complexes.

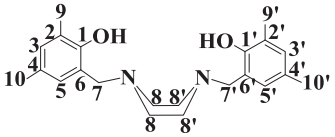

Compound[a]	C_1/C_1'	C_2/C_2'	C_3/C_3'	C_4/C_4'	C_5/C_5'	C_6/C_6'	C_7/C_7'	C_8/C_8'	C_9/C_9'	C_{10}/C_{10}'
H_2Pip-2,4-dmp	153.4	123.9	131.0	129.8	127.3	121.0	52.6	52.3	16.1	20.6
[$Mo^{VI}O_2$(pip-2,4-dmp)] (Δδ)	153.3 (−0.1)	121.8	133.9	128.3	127.6	117.5 (−3.5)	60.5 (7.9)	54.7 (2.4)	16.2	20.6
[$U^{VI}O_2$(pip-2,4-dmp)(MeOH)] (Δδ)	164.9 (11.5)	124.8	131.1	127.7	126.7	124.0 (3.0)	60.7 (8.1)	53.0 (0.7)	17.3	20.5

[a] Δδ = [δ (complex) − δ(free ligand)].

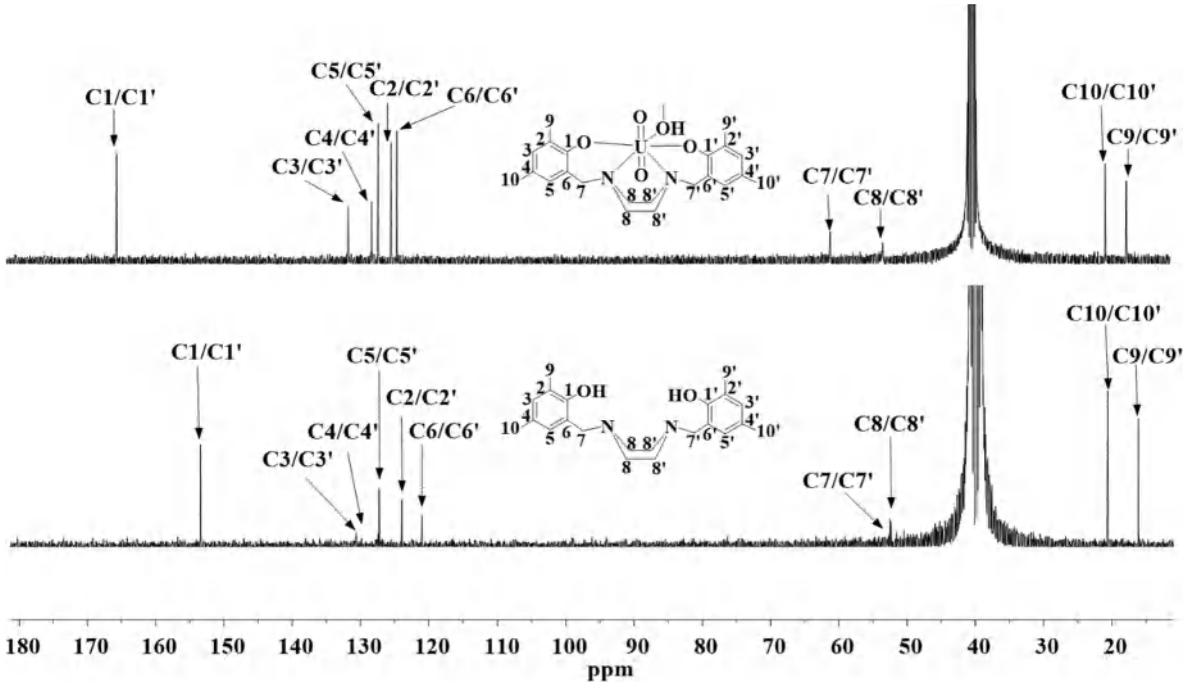

Fig. 3. ^{13}C NMR spectra of H_2pip-2,4-dmp (**I**) and [$U^{VI}O_2$(pip-2,4-dmp)(MeOH)] (**2**).

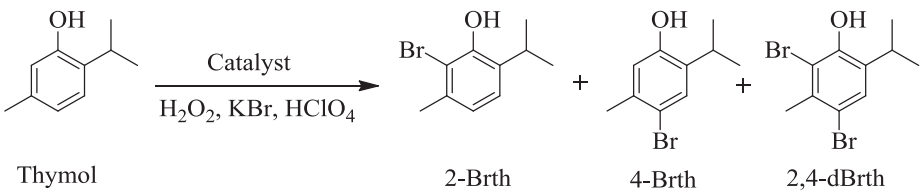

Scheme 2. Products of the oxidative bromination of thymol. 2-Brth = 2-bromothymol, 4-Brth = 4-bromothymol, 2,4-dBrth = 2,4-dibromothymol.

To obtain the maximum yield of brominated products for both the catalysts, several parameters, such as, amounts of catalyst, 30% H_2O_2, KBr, and 70% $HClO_4$, were varied separately for both of them at room temperature. We have first optimized the reaction conditions considering different amounts of catalyst, H_2O_2, KBr and $HClO_4$ using [$Mo^{VI}O_2$(pip-2,4-dmp)] (**1**) as a catalyst. Thus, for 10 mmol (1.50 g) of thymol, three different amounts of catalyst viz. 0.001, 0.002 and 0.003 g and 1:1, 1:2 and 1:3 ratios each for substrate:H_2O_2, substrate:KBr and substrate:$HClO_4$ were taken in 20 mL water and the reaction was carried out at room temperature for 2 h. It was observed that $HClO_4$ added at a time in case of 20 and 30 mmol led to the partial decomposition of catalyst, therefore, in these cases $HClO_4$ was added in two and three equal portions, respectively, to the reaction mixture, first portion at t = 0 and other one/two portions after every 30 min intervals. Figs. 4–7 present time on analysis for different conditions and Table 7 summarizes details of all reaction conditions and the conversion of thymol at 2 h of reaction time.

As accessible in Table 7, the optimized reaction condition for the maximum conversion of 10 mmol (1.50 g) of thymol using **1** as catalyst is as presented in entry 8 i.e. those using catalyst:H_2O_2:KBr:$HClO_4$ ratios (in mmol) of $10{:}4.16 \times 10^{-3}{:}10{:}20$. Under these conditions a maximum of 99% conversion of thymol was achieved where products 2-bromothymol, 4-bromothymol and 2,4-dibromothymol with the percentage selectivity of 1, 2 and 97, respectively were obtained. Turn over frequency calculated at 2 h of reaction is 1198 h^{-1} for this condition. Higher amount of KBr (30 mmol) and lower amount of acid (10 mmol) favors the formation of monobromo derivatives (see entry 7) to some extent while higher amount of acid (30 mmol) and lower amount (10 mmol) of KBr favors the formation of dibromo derivative (entry 9). However, at any reaction conditions (Table 7), the yield of 2,4-dimromo derivative is always higher. Further, no trace of substrate was observable in GC profile under the conditions mentioned in entry 9 of Table 7, suggesting the complete conversion of thymol to products. Blank reaction i.e. without catalyst but in the presence of

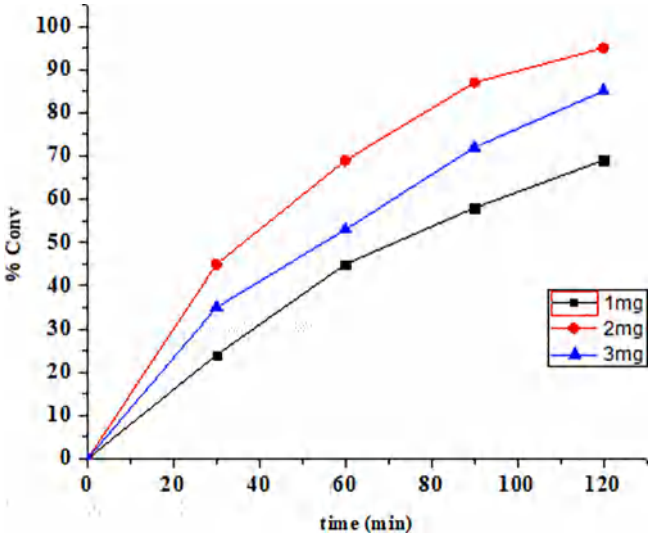

Fig. 4. Conversion of 10 mmol of thymol with varying amounts of [$Mo^{VI}O_2$(pip-2,4-dmp)]. Other reaction conditions (in mmol), substrate:H_2O_2:KBr:$HClO_4$ ratios of 10:10:10:10.

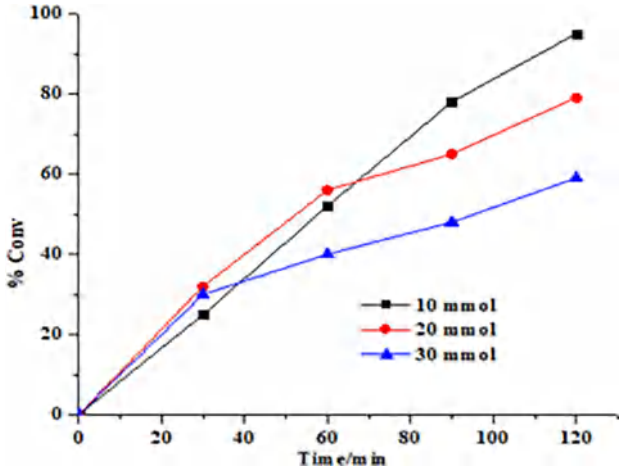

Fig. 5. Effect of oxidant on the oxidative bromination of 10 mmol of thymol using [$Mo^{VI}O_2$(pip-2,4-dmp)] as catalyst. Other reaction conditions (in mmol), substrate:catalyst:KBr:$HClO_4$ ratios of 10:4.16 × 10^{-3}:10:10.

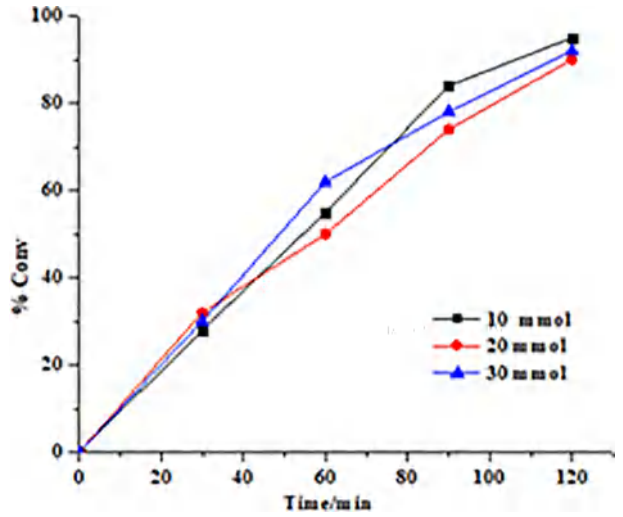

Fig. 6. Effect of variation of KBr on the oxidative bromination of thymol using [$Mo^{VI}O_2$(pip-2,4-dmp)] complex as catalyst. Other reaction conditions (in mmol), substrate:oxidant:catalyst:$HClO_4$ ratios of 10:10:4.16 × 10^{-3}:10.

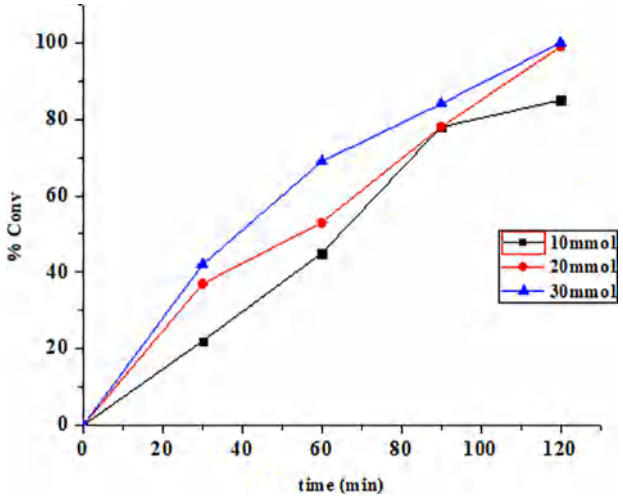

Fig. 7. Effect of variation of $HClO_4$ on the oxidative bromination of thymol using [$Mo^{VI}O_2$(pip-2,4-dmp)] complex as catalyst. Other reaction conditions (in mmol), substrate:oxidant:catalyst:KBr ratios of 10:10:4.16 × 10^{-3}:10:10.

substrate:H_2O_2:KBr:$HClO_4$ ratios (in mmol) of 10:10:10:20, a maximum of 45% conversion was noted, therefore the catalyst enhances the conversion of thymol.

We have also optimized all reaction parameters mentioned above in 20 mL water for catalyst **2**. In this case also reaction acquires equilibrium in 2 h of reaction time at room temperature. Figs. 8–11 present time on analysis of conversion of thymol under various reaction conditions and Table 8 summarizes all the reactions conditions studied and the corresponding percentage of oxidative bromination of thymol along with TOF and the selectivity of different reaction products. Data presented in Table 8 again prove that the conversions and the selectivity of products differ on varying the reagents and the best reaction conditions (entry 10) for the maximum oxidative bromination of 10 mmol of thymol with 92% conversion are: catalyst (0.003 g, 4.8 × 10^{-3} mmol), H_2O_2 (3.39 g, 30 mmol), KBr (1.19 g, 10 mmol) and $HClO_4$ (4.29 g, 30 mmol) in 20 mL water i.e. substrate:oxidant:catalyst:KBr:$HClO_4$ ratios (in mmol) of 10:30:4.8 × 10^{-3}:10:30. Under these conditions, only two products, 4-bromothymol and 2,4-bibromothymol with the selectivity percent of 1 and 99% were obtained. Turn over frequency calculated at 2 h under this condition is 956 which is much less than that obtained for molybdenum catalyst. The overall conversion is also less than molybdenum complex.

The catalytic oxidative bromination of uranium complex is relatively low but of molybdenum complex reported here is very well comparable with those reported for dioxidomolybdenum(VI) complexes (94–99%) of Schiff base ligands derived from 8-formyl-7-hydroxy-4-methylcoumarin and hydrazides [17]. However, the selectivity of 2,4-dibromothymol varies within these two complexes reported here as well as within those reported in literature. The vanadium complex [$V^{V}O$(OMe)(MeOH)(L)] [H_2L = 6,6′-(2-(pyridin-2-yl)ethylazanediyl)bis(methylene)bis(2,4-di-*tert*-butylphenol)] under the optimised reaction conditions (i.e. substrate:H_2O_2:KBr:$HClO_4$ of 1:2:2:2 for 10 mmol of thymol) gave as high as 99% conversion with 57% selectivity towards 2,4-dibromothymol, followed by 37% towards the 4-bromothymol and rest towards 2-bromothymol isomer [35]. Complexes, [$W^{VI}O_2$(hap-hyz)(MeOH)] (H_2hap-hyz = Schiff bases derived from 2-hydroxy acetophenone and hydrazides) show conversion between 91 and 96% [36] which is again better than uranium complex but almost same like molybdenum complex.

3.8. Reactivity of uranium complex with H_2O_2 and possible reaction mechanism

As observed in *cis*-[MO_2]-complexes (M = V, Mo) [21,37], KBr in the presence of H_2O_2 and $HClO_4$, catalytically generate HOBr and/or Br^+, Br_2, which are the brominating reagent for the substrates. Conte *et al.* have identified an oxidomonoperoxidovanadium(V) complex as the oxidant of the Br^- ion to HOBr/Br_2 by spectroscopic techniques [38]. It was also observed recently by ^{51}V NMR study that the [$VO(O_2)$(L)]-type species is an active intermediate during catalytic study of oxidative bromination of thymol in the presence of oxidant H_2O_2 [35]. In order to generate information for such an intermediate in *trans*-[UO_2]-complexes, we have also treated uranium complex **2** with H_2O_2 and monitored the changes by UV–Vis spectroscopy. Thus, the successive addition of one drop portion of 30% H_2O_2 (0.108 g, 0.95 mmol) dissolved in 5 mL of MeCN to 25 mL of 4.8 × 10^{-3} M solution of **2** in MeCN resulted in the continuous decrease in the intensity of 502 and 383 nm bands to almost flat (Fig. 12). The UV region (not shown here) is not much affected. These spectral changes suggest the reaction of H_2O_2 with uranium complex and the formation of possibly peroxido species in solution. Such peroxido intermediate, as observed in vanadium and molybdenum complexes, is responsible for the generation of brominating reagent from KBr catalytically.

Table 7
Conversion of 10 mmol (1.50 g) of thymol using [$Mo^{VI}O_2$(pip-2,4-dmp)] complex as a catalyst precursor for 2 h of reaction time under different reaction conditions.

Sr. No.	KBr [g (mmol)]	H_2O_2 [g (mmol)]	$HClO_4$ [g (mmol)]	Catalyst [mg (mmol)]	Conv. (%)	TOF	2-Brth	4-Brth	2,4-dBrth
1	1.19 (10)	1.13 (10)	1.43 (10)	1.0 (2.08×10^{-3})	69	1658	10	22	67
2	1.19 (10)	1.13 (10)	1.43 (10)	2.0 (4.16×10^{-3})	95	1141	10	21	69
3	1.19 (10)	1.13 (10)	1.43 (10)	3.0 (6.24×10^{-3})	85	681	10	33	57
4	1.19 (10)	2.27 (20)	1.43 (10)	2.0 (4.16×10^{-3})	79	949	12	18	69
5	1.19 (10)	3.39 (30)	1.43 (10)	2.0 (4.16×10^{-3})	59	709	10	29	59
6	2.38 (20)	1.13 (10)	1.43 (10)	2.0 (4.16×10^{-3})	90	1081	8	17	73
7	3.57 (30)	1.13 (10)	1.43 (10)	2.0 (4.16×10^{-3})	92	1105	16	24	59
8	1.19 (10)	1.13 (10)	2.86 (20)	2.0 (4.16×10^{-3})	99	1189	1	2	97
9	1.19 (10)	1.13 (10)	4.29 (30)	2.0 (4.16×10^{-3})	100	1201	–	1	99
10	1.19 (10)	1.13 (10)	4.29 (30)	–	45	–	35	5	60

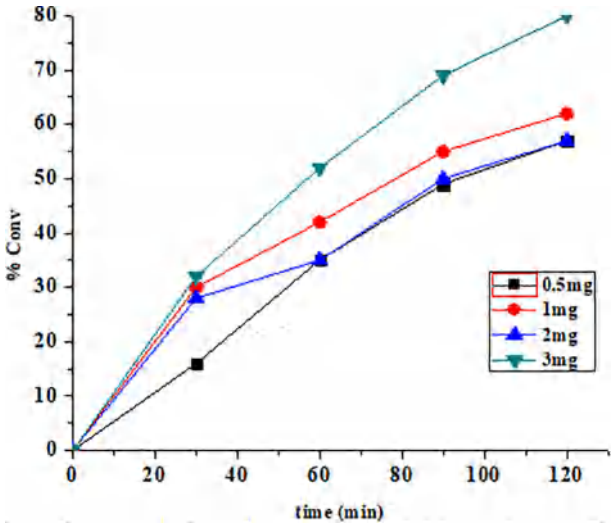

Fig. 8. Conversion of thymol with varying amounts of [$U^{VI}O_2$(pip-2,4-dmp)(MeOH)] as catalyst. Other reactions, Other reaction conditions (in mmol), substrate:H_2O_2:KBr:$HClO_4$ ratios of 10:10:10:10.

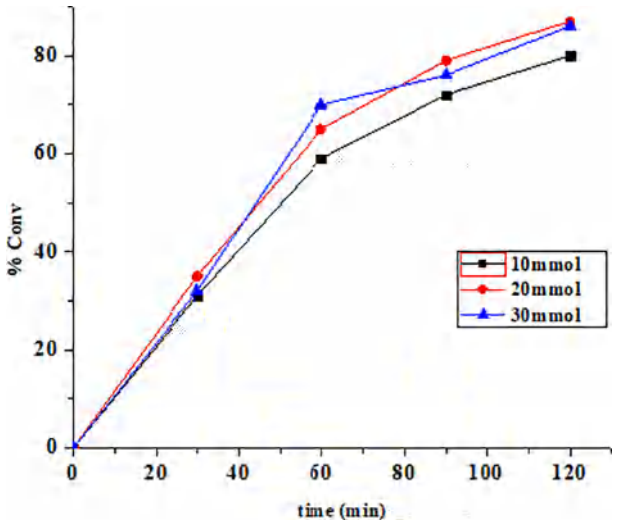

Fig. 10. Effect of variation of KBr on the oxidative bromination of thymol using [$U^{VI}O_2$(pip-2,4-dmp)(MeOH)] as catalyst. Other reaction conditions (in mmol), substrate:catalyst:KBr:$HClO_4$ ratios of $10{:}4.8 \times 10^{-3}{:}\ 10{:}10$.

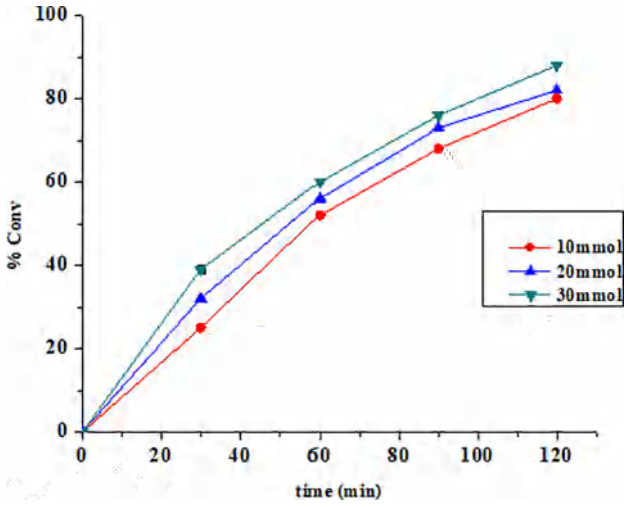

Fig. 9. Effect of oxidant on the oxidative bromination of thymol using [$U^{VI}O_2$(pip-2,4-dmp)(MeOH)] as a catalyst. Other reaction conditions (in mmol), substrate:catalyst:KBr:$HClO_4$ ratios of $10{:}4.8 \times 10^{-3}{:}\ 10{:}10$.

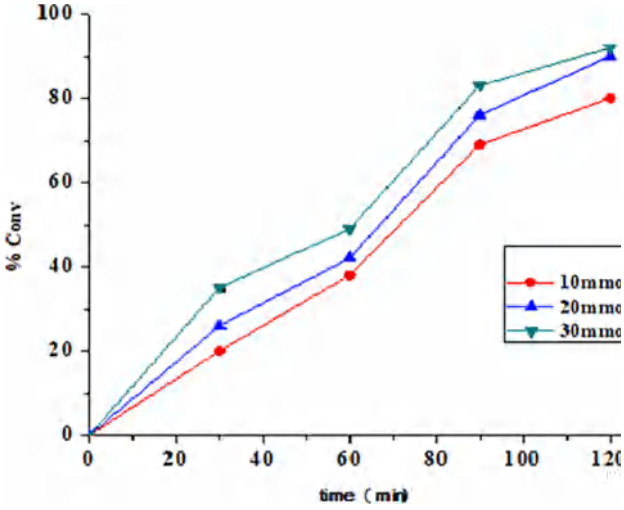

Fig. 11. Effect of variation of $HClO_4$ on the oxidative bromination of thymol using [$U^{VI}O_2$(pip-2,4-dmp)(MeOH)] complex as catalyst. Other reaction conditions (in mmol), substrate:oxidant:catalyst:KBr ratios of $10{:}4.8 \times 10^{-3}{:}\ 10{:}10$.

4. Conclusions

Dioxidomolybdenum (VI) and dioxidouranium (VI) complexes of piperazine derived tetradentate (O,N,N,O) donor ligand, bis{(2,4-dmp)CH_2}(μ_2-piperazine)] (H_2pip-2,4-dmp) were prepared successfully and characterized by UV, IR, NMR, elemental analysis and TGA, and single crystal X-ray study of uranium complex. Based on the characterization data it has been concluded that molybdenum in complex [$Mo^{VI}O_2$(pip-2,4-dmp)] is *hexa*-coordinated while uranium in [$U^{VI}O_2$(pip-2,4-dmp)(MeOH)] is hepta-coordinated. The catalytic activity of these complexes for the oxidative bromination of thymol, a

Table 8
Conversion of 10 mmol (1.5 g) thymol using $[U^{VI}O_2(pip\text{-}2,4\text{-}dmp)(MeOH)]$ as a catalyst for 2 h of reaction time under different reaction conditions.

Sr. No.	KBr [g (mmol)]	H_2O_2 [g(mmol]	$HClO_4$ [g(mmol)]	Catalyst [mg (mmol)]	Conv (%)	TOF (h^{-1})	2-Brth	4-BrTh	2,4-dBrth
1	1.19 (10)	1.13 (10)	1.43 (10)	0.5 (8.03×10^{-4})	57	3549	13	4	82
2	1.19 (10)	1.13 (10)	1.43 (10)	1.0 (1.60×10^{-3})	62	1937	10	9	80
3	1.19 (10)	1.13 (10)	1.43 (10)	2.0 (3.2×10^{-3})	57	890	11	3	85
4	1.19 (10)	1.13 (10)	1.43 (10)	3.0 (4.8×10^{-3})	80	831	6	14	78
5	1.19 (10)	2.27 (20)	1.43 (10)	3.0 (4.8×10^{-3})	82	852	13	15	71
6	1.19 (10)	3.39 (30)	1.43 (10)	3.0 (4.8×10^{-3})	88	914	8	43	48
7	2.38 (20)	3.39 (30)	1.43 (10)	3.0 (4.8×10^{-3})	87	904	4	17	78
8	3.57 (30)	3.39 (30)	1.43 (10)	3.0 (4.8×10^{-3})	86	893	10	18	72
9	2.38 (20)	3.39 (30)	2.86 (20)	3.0 (4.8×10^{-3})	90	935	–	4	96
10	2.38 (20)	3.39 (30)	4.29 (30)	3.0 (4.8×10^{-3})	92	956	–	1	99
12	2.38 (20)	3.39 (30)	4.29 (30)	–	42		35	31	44

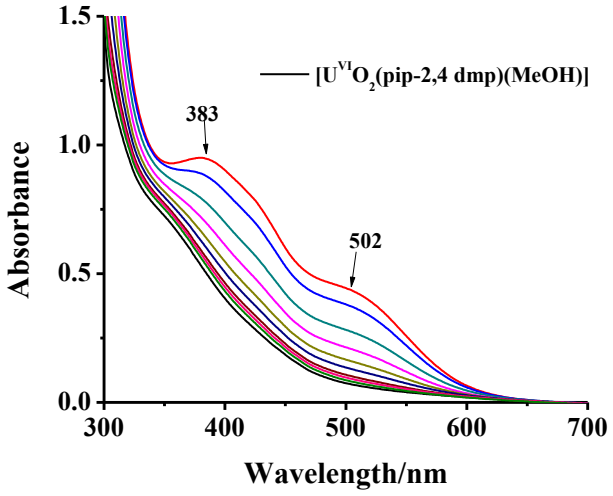

Fig. 12. Plots representing the spectral changes observed during the titration of $[U^{VI}O_2(pip\text{-}2,4\ dmp)(MeOH)]$ (**2**) with H_2O_2. Spectra were obtained after successive addition of one drop portion of 30% H_2O_2 (0.108 g, 0.95 mmol) dissolved in 5 mL of MeCN to 25 mL of 4.8×10^{-3} M solution of **2** in MeCN.

reaction generally observed by vanadium dependent haloperoxidases, was studied by gas chromatography and it has been observed that these complexes show very good conversion and enhanced selectivity towards the products in the order: 2,4-dibromothymol > 4-bromothymol > 2-bromothymol, under the optimized reaction conditions. Thus, these complexes mimic similar catalytic reactivity as shown by vanadium based haloperoxidases.

Acknowledgment

B.M. is thankful to the Federal Democratic Republic of Ethiopia, Ministry of Education, Addis Ababa, for scholarship.

Appendix A. Supplementary data

Supplementary data to this article can be found online at https://doi.org/10.1016/j.ica.2018.11.031.

References

[1] R. Hille, Trend Biochem. Sciences 27 (2002) 360–367.
[2] K. Heinze, Coord. Chem. Rev. 300 (2015) 121–141.
[3] N. Baig, V.K. Madduluri, A.K. Sah, RSC Adv. 6 (2016) 28015–28022.
[4] M.R. Maurya, Curr. Org. Chem. 16 (2012) 73–88.
[5] M. Afsharpour, A.R. Mahjoub, M.M. Amini, Appl. Catal. A: Gen. 327 (2007) 205–210.
[6] M.M. Farahani, F. Farzaneh, M. Ghandi, Catal. Commun. 8 (2007) 6–10.
[7] M. Bagherzadeh, R. Latifi, L. Tahsini, V. Amani, A. Ellern, L.K. Woo, Polyhedron 28 (2009) 2517–2521.
[8] A. Rezaeifard, I. Sheikhshoaie, N. Monadi, M. Alipour, Polyhedron 29 (2010) 2703–2709.
[9] A.C. Coelho, M. Nolasco, S.S. Balula, M.M. Antunes, C.C.L. Pereira, F.A.A. Paz, A.A. Valente, M. Pillinger, P. Ribeiro-Claro, J. Klinowski, I.S. Goncalves, Inorg. Chem. 50 (2011) 525–538.
[10] A. Majumdar, S. Sarkar, Coord. Chem. Rev. 255 (2011) 1039–1054.
[11] J. Pisk, D. Agustin, V. Vrdoljak, R. Poli, Adv. Synth. Catal. 353 (2011) 2910–2914.
[12] J. Pisk, B. Prugovečki, D. Matković-Čalogović, R. Poli, D. Agustin, V. Vrdoljak, Polyhedron 33 (2012) 441–449.
[13] M.E. Judmaier, C. Holzer, M. Volpe, N.C. Mösch-Zanetti, Inorg. Chem. 51 (2012) 9956–9966.
[14] S. Rayati, N. Rafiee, A. Wojtczak, Inorg. Chim. Acta 386 (2012) 27–35.
[15] X. Lei, N. Chelamalla, Polyhedron 49 (2013) 244–251.
[16] M.R. Maurya, L. Rana, F. Avecilla, New J. Chem. 41 (2017) 724–734.
[17] M.R. Maurya, N. Saini, F. Avecilla, RSC Adv. 6 (2016) 101076–101088.
[18] K. Jeyakumar, D.K. Chand, J. Chem. Sci. 121 (2009) 111–123.
[19] M. Bagherzadeh, M.M. Haghdoost, M. Amini, P.G. Derakhshandeh, Catal. Commun. 23 (2012) 14–19.
[20] R.D. Chakravarthy, K. Suresh, V. Ramkumar, D.K. Chand, Inorg. Chim. Acta 376 (2011) 57–63.
[21] M.R. Maurya, S. Dhaka, F. Avecila, Polyhedron 96 (2015) 79–87.
[22] M.R. Maurya, A.A. Khan, A. Azam, S. Ranjan, N. Mondal, A. Kumar, F. Avecilla, J.C. Pessoa, Dalton Trans. 39 (2010) 1345–1360.
[23] M.R. Maurya, N. Kumar, F. Avecilla, J. Mol. Catal. A: Chem. 392 (2014) 50–60.
[24] G.J. Colpas, B.J. Hamstra, J.W. Kampf, V.L. Pecoraro, J. Am. Chem. Soc. 118 (1996) 3469–3478.
[25] M.R. Maurya, N. Chaudhary, A. Kumar, F. Avecilla, J.C. Pessoa, Inorg. Chim. Acta 420 (2014) 24–38.
[26] M.R. Maurya, A. Kumar, M. Ebel, D. Rehder, Inorg. Chem. 45 (2006) 5924–5937.
[27] M.R. Maurya, R.C. Maurya, Rev. Inorg. Chem. 15 (1995) 1–107.
[28] (a) C.C. Gattoa, E.S. Langa, A. Kupferb, A. Hagenbachb, U. Abram, Z. Anorg, Allg. Chem. 630 (2004) 1286–1295;
(b) R. Takjoo, A. Najafi, S.W. Ngb, E.R.T. Tiekink, Acta Cryst. E68 (2012) m255–m256;
(c) M. Şahin, N. Ozdemir, T. Bal-Demirci, B. Ulkuseven, M. Dincer, M.S. Soylu, Spectrochim Acta Part A: Mol. Biomol. Spectrosc. 135 (2015) 994–1001;
(d) Y. Zhang, D.J. Fanna, N.D. Shepherd, I. Karatchevtseva, K. Lu, L. Konga, J.R. Price, RSC Adv. 6 (2016) 75045–75053;
(e) A. Akbari, A. Fasihizad, M. Ahmadi, B. Machura, Polyhedron 128 (2017) 188–197.
[29] (a) M. Ephritikhine, Dalton Trans. (2006) 2501–2516;
(b) S.C. Bart, K. Meyer, Struct. Bond. 127 (2008) 119–176.
[30] G.J.J. Chen, J.W. McDonald, W.E. Newton, Inorg. Chem. 15 (1976) 2612–2615.
[31] S. Mohanty, D. Suresh, M.S. Balakrishna, J.T. Mague, J. Organometal. Chem. 694 (2009) 2114–2121.
[32] G.M. Sheldrick, SADABS, Version 2.10, University of Göttingen, Germany, 2004.
[33] (a) O.V. Dolomanov, L.J. Bourhis, R.J. Gildea, J.A.K. Howard, H. Puschmann, J. Appl. Cryst. 42 (2009) 339–341;
(b) G.M. Sheldrick, SHELXL, Acta Crystallogr., Sect. C 71 (2015) 3–8.
[34] S.T. Tsantis, V. Bekiari, C.P. Raptopoulou, D.I. Tzimopoulos, V. Psycharis, S.P. Perlepes, Polyhedron 152 (2018) 172–178.
[35] M.R. Maurya, B. Uprety, F. Avecilla, P. Adão, J. Costa Pessoa, Dalton Trans. 44 (2015) 17736–17755.
[36] M.R. Maurya, L. Rana, F. Avecilla, Inorg. Chim. Acta 440 (2016) 172–180.
[37] M.R. Maurya, C. Haldar, A. Kumar, M.L. Kuznetsov, F. Avecillac, J. Costa Pessoa, Dalton Trans. 42 (2013) 11941–11962.
[38] V. Conte, B. Floris, Inorg. Chim. Acta 363 (2010) 1935–1946.